Regional Air-Sea Interactions (RASI) Climatology for Central America Coastal Gap Wind and Upwelling Events

Deborah K. Smith
Remote Sensing Systems
Santa Rosa, CA, USA
smith@remss.com

Xiang Li, Ken Keiser, Shannon Flynn
Information Technology and Systems Center
University of Alabama in Huntsville
Huntsville, AL, USA

***Abstract*— Coastal gap wind jets and associated ocean upwelling events present significant regional Air-Sea interaction over the eastern Pacific warm pool. Besides the regional weather impact, the ocean upwelling events also significantly change the nutrient distribution over the area by bringing up deep cold water and nutrients to the ocean surface. These events are therefore of interest to both research and commercial users. In this paper, we present automated algorithms to extract gap wind and upwelling events from satellite-derived data products. An ocean upwelling event is characterized by a sudden and significant decrease in sea surface temperature (SST). This study focuses on three special locations: the Gulf of Tehuantepec, Gulf of Papagayo and Gulf of Panama, where gap wind events are often observed during northern hemisphere winter months. The information acquired from this automated detection is collected and managed by the Global Hydrology Resource Center (GHRC), a NASA Distributed Active Archive Center (DAAC), located in Huntsville, AL, and is made publicly available to users.**

Keywords—gap winds, upwelling, automated event detection

I. INTRODUCTION

Coastal gap wind jets over the Gulfs of Tehuantepec, Papagayo and Panama located in Central America and associated cold water ocean upwelling presents significant air-sea interaction scenarios over the eastern Pacific warm pool. These low level regional wind jets result from the interaction between large scale atmospheric systems and local orographic effects. In describing our methodology, we will focus on the Gulf of Tehuantepec where the Tehuano gap wind is triggered by cold air outbreaks that originate over the Great Plains of North America. The pressure differences across the Chivela Pass, a narrow gap in the Sierra Madre mountain range, cause high wind speeds in excess of 20 m/s. This gap wind jet can extend hundreds of kilometers out into the Gulf of Tehuantepec and beyond into the Pacific [1]. Large pressure gradients due to cold air outbreaks as well as the trade winds are the mechanisms that produce wind jets that blow through mountain gaps and into the other two regions, the Gulfs of Papagayo and Panama [2].

Strong wind jets can produce associated cold water upwelling by triggering intense vertical mixing of the ocean. With cold water upwelling, warm surface water is pushed by the wind jet away from the coast and deep cold water and nutrients rise to the surface. This process significantly changes the regional nutrient distribution and the local ecological environment [9, 15].

Studies of the gap wind events date back to the 1920s [3, 4], but with the advent of satellite measurements, researchers could begin to study these features from space [5, 6, 7]. However, it is the latest advances in microwave wind products that offer the means for detailed wind jet studies due to the through-cloud capabilities of both microwave radiometers and scatterometers. Previous work of this sort includes case studies by Chelton et al in which they studied the Central American wind jets using NASA scatterometer winds (NSCAT) to determine statistical characteristics [1] and regional relationships [8]. However, the NSCAT instrument only operated for 9 months, so no long-term study was performed.

Xie et al [9] examined the gap wind induced air-sea interaction over the eastern Pacific warm pool, using microwave SSTs, winds from QuikSCAT, and SeaWiFS ocean color and chlorophyll concentrations. Their study found that orographic-triggered air–sea interaction may have long-lasting effects in both the ocean and atmosphere. They also suggested that documentation of orographically-induced air-sea coupled phenomena can serve as a benchmark for accurately evaluating coupled atmospheric-ocean models. Their work indicates the importance of establishing a gap wind and ocean upwelling climatology.

The study most similar to the work presented here is that by Brennan et al. in which they used 25 km QuikSCAT winds to deduce 10-year climatology of gale- and storm-force Tehuano wind events [10]. They used a thresholding technique to detect the gap wind events with thresholds set at 34 kt (gale) and 48 kt (storm) levels. The resulting climatology contained 119 gale- and 64 storm-force events observed for the cold seasons (Oct to May) from 1999 to 2009, resulting in an average of 11.9 gale-force and 6.4 storm-force events per cold season. When 12.5 km QuikSCAT winds became available after 2003, they found the average number of storms increased from 6.4 to 8.1 per cold season. We will examine our results to see if they compare with those from Brennan et al.

The Brennan et al. [10] studies were only performed on the Gulf of Tehuantepec wind jet. The advantage of our automated approach is that we can determine the climatology of these

This research effort is conducted as part of DISCOVER (Distributed Information Services for Climate and Ocean Products and Visualization for Earth Research), a NASA/MEaSUREs project.

wind events for all three Gulf regions with the potential of expanding the time period to the full operational time of microwave radiometers (1987 to present).

The methods we have developed for automatically identifying gap wind and ocean upwelling events in the three gulf regions have been previously presented [11], however, more recent changes and improvements will be presented here. In our previous work, we focused on the detection of the occurrence of wind jet events. In our latest development, we extract the most significant wind jet regions (core wind jet regions). These regions more accurately reflect the location and spatial coverage of the gap wind events. A wind jet is normally identified as an elongated region with cross-stream width significantly narrower than the along-stream distance. In the updated algorithm, a couple of shape factors are applied to reinforce the shape constraint so that extracted wind regions are more representative. The new methodology is described in Section III and results of our improved methods are presented in Section IV.

II. Data Description

We need to use consistently processed, complete (no data gaps), high quality data for the automated methods we have developed. Since we want to identify local features, the data products need to have better resolution than global weather model output as it is known that the features are often not located in model data [12]. In this study, we use two data products produced using satellite data of winds over the ocean and sea surface temperatures.

The wind product is the Cross-Calibrated Multi-Platform ocean surface winds (CCMP, [13]). This wind product combines wind measurements from SeaWinds on QuikSCAT, AMSR-E (Advanced Microwave Scanning Radiometer for EOS on Aqua), TRMM TMI (Tropical Rainfall Measuring Mission's Microwave Imager), and both SSM/I (Special Sensor Microwave/Imager) and SSMIS (Special Sensor Microwave/Imager Sounder) on DMSP satellites using a 4D variational analysis method (VAM). See Atlas et al [13] for details. The data are available from the NASA PO-DAAC (http://podaac.jpl.nasa.gov/) and contains global high resolution (25 km) ocean surface winds for the period July 1987 through 2011. Our study uses the Level 3.0 First-Look (FLK) data that contain 6-hourly gridded VAM analyses at time steps of 0, 6, 12 and 18 Z. We use only fourteen years of the CCMP data (1998 to 2011) because the SST data that are also analyzed are not available until 1998 once TMI was launched.

The SST data are the Microwave Optimally Interpolated Sea Surface Temperatures (OISST) data set from Remote Sensing Systems [14] (http://www.remss.com/sst/). This product is created using SSTs from TMI, AMSR-E and WindSat measurements which are combined into daily, diurnally corrected files using an optimal interpolation technique. These daily SSTs are available on a 0.25 degree Earth grid from 1998 to present. The SSTs incorporated from TMI exist only for 40N to 40S latitude, while the AMSR-E and WindSat SSTs have near-global coverage. This means the OI product in the early years (1997 to 2001 when only TMI was available) has limited spatial coverage. However for this study region, this limitation is not an issue. These optimally interpolated satellite SST measurements are diurnally corrected and represent a daily 12 noon foundation SST. We use data from 1998 to 2009 for this study.

III. Detection Methods

A. Gap Wind Detection

Our goal was to develop an automated means of identifying the location, shape, size, and intensity of gap wind events in the CCMP ocean wind data. Since CCMP data are organized into 6-hourly maps, we must first determine whether gap winds are present in each CCMP map and then carefully combine these outcomes to determine the temporal and spatial extent of a single gap wind event. A trained scientist can fairly easily identify the presence of a gap wind in one map and can also identify the start and end of the event by examining successive maps. However, transferring what the human can easily do to an automated identification method is not a simple task. The methodology we used to automatically identify gap winds from the satellite-based CCMP data includes the steps described below. More detail about the steps than what is described here can be found in the algorithm documentation at (https://ghrc.nsstc.nasa.gov/rasi/main.php).

Hierarchical thresholding is used to identify gap winds in individual CCMP wind maps. A hierarchical thresholding algorithm applies a hierarchy of connected processing steps such as iterating over a range of threshold values, to narrow down solution space for optimal solutions. Hierarchical methods have been successfully used to improve thresholding and segmentation performances in complex image scenes [15, 16, 17]. Our hierarchical thresholding is an iterative process, starting with an upper bound value (highTH) of the threshold range and decreases the threshold value by a certain decrement at each step (currently defined as 0.1 m/s), ending when either the lower threshold value (lowTH) is reached or one or more terminating conditions are met. The highTH and lowTH values are determined for each individual map. Several conditions are used to constrain the hierarchical thresholding process. For a region to qualify as a gap wind, a minimum wind region size is required in order to exclude any trivial occurrences of high winds that may be due to data uncertainty or other meteorological features. A maximum wind region size is also defined so that only the wind jet is detected. Several other factors are also used as constraints, including the shape of the high wind region identified, the wind speed gradients found in the map, any significant changes in size from one step to another, and the detection of multiple regions that merge. Note the difference of this hierarchical thresholding method as compared to our previous version. In Li et al [11], hierarchical thresholding started with a low threshold value and increased iteratively. The thresholding process terminated when region size was below the maximum region size allowed. In other words, the process was only constrained by the size of the detected region without shape considerations. As a result, detected regions were often of irregular shapes and large in size for strong events.

The following paragraphs describe the steps of the gap wind identification algorithm in detail. For each of the steps below, we refer the reader to Fig. 1, which shows the location of the specific regions mentioned for the Gulf of Tehuantepec example.

Step 1: Determine the upper and lower bounds for an individual map

The highTH of the thresholding range is calculated as the maximum wind speed for the expected gap wind initiation region, shown as the black box close to the coast in Fig. 1. The lowTH value is determined using the following four conditions: 1) The lowTH is no less than the location-dependent minimum speed threshold minTH value, which is empirically-defined for each of the three locations in the study (e.g. set as 7.0 m/s for Tehuantepec). 2) The lowTH is no less than the calculated Otsu threshold value [18] using the wind data in the SmallArea, illustrated as a black bounding box in Fig. 1. The Otsu threshold separates grid cells into the ones with weak wind speeds and those with strong wind speeds. 3) The lowTH is no less than a value 2.0 m/s higher than the highest wind speed at the two reference locations (red squares in Fig. 1). The winds at these reference locations represent neighboring wind conditions outside the expected gap wind region. 4) The lowTH is no more than 9.0 m/s except for a few very strong events such as gale-scale (≥34 kt) and storm-scale (≥48 kt) gap wind events.

Step 2: Detect steep wind speed gradients

We expect significant changes in wind speed (high wind gradients) near the boundaries of a gap wind. By using an edge detection algorithm, we identify the wind gradient edges in each map. We use the Canny Edge Detection algorithm [19] which is a well-known image processing algorithm to detect edges in images using a multi-step process. The Canny method produces a number of edge segments. If a gap wind exists in the map, the largest edge segments will exist near the gulf mouth where the high winds blow offshore from the mountain gap. The edge information is then used as a constraint to the thresholding process (Step 3). We find that optimal gap wind identification occurs when the gap wind boundary meets the strongest speed gradients, as illustrated in Fig. 1, in which the two blue lines represent the wind speed gradient locations and the orange oval represents the identified gap wind region.

Step 3: Perform hierarchical thresholding to locate a gap wind region

In this step, we perform the hierarchical thresholding to identify gap winds within individual CCMP maps. Wind gradient information from Step 2 and other constraints are used as terminating conditions for the hierarchical thresholding process. The thresholding process starts with the highTH value obtained in the SmallArea where gap winds initiate (black box in Fig. 1). In subsequent steps, the threshold is decremented until one of the constraints is met or the lowTH value is

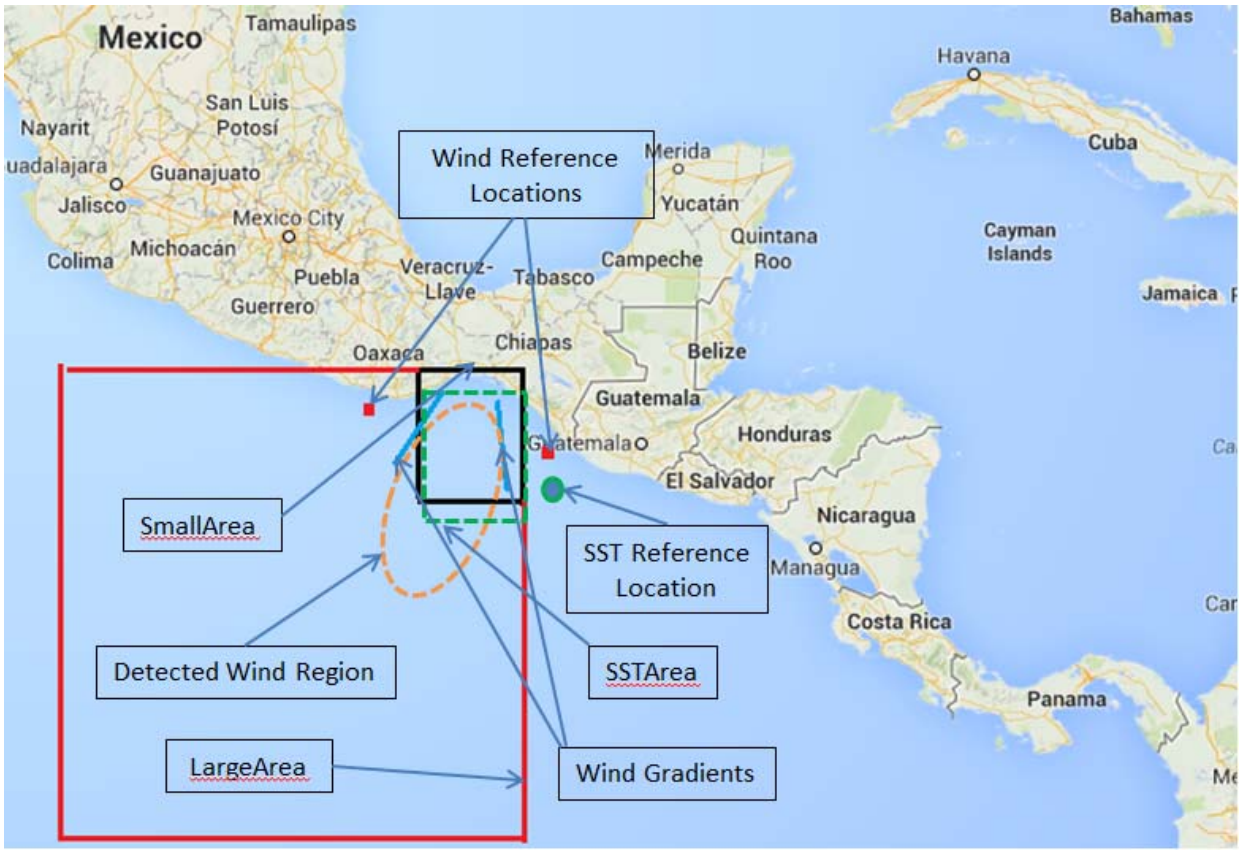

Fig. 1: Illustration of sample regions and reference points used in the analysis of gap wind and SST events in Gulf of Tehuantepec.

reached.

We begin the detection process in the SmallArea to make sure that if high winds are identified, they are most likely in the expected gap wind region. The detected region size increases with subsequent iterations as the threshold decreases. A minimum of 9 grid cells in the SmallArea is required in order for the process to transition to the large area. This requirement prevents spurious or trivial high winds from being falsely detected. A grid cell in the CCMP map covers an Earth surface area of approximately 0.25 degree latitude by 0.25 degree longitude. Once the detected area transitions to the LargeArea, the hierarchical thresholding process then continues until the entire region is identified as determined by the ending conditions. We refer readers to the algorithm description document (https://ghrc.nsstc.nasa.gov/rasi/main.php) for more details of hierarchical thresholding process. We expect the largeArea, which encompasses the smallArea shown in Fig. 1, to contain most of the gap wind. The largeArea for each study location was defined by looking at years of gap wind events in satellite data for each study location.

Step 4: Post processing of identified gap wind region

To smooth the potential irregularity of the wind jet boundary detected in Step 3, the convex hull of the area is used to replace the detected area. Common image morphological open and close operations [20] are further applied in sequence to smooth the boundaries and to fill any potential small holes that may exist within the detected wind region.

Step 5: Apply wind direction criterion

To qualify as a gap wind, the wind direction of the identified region must also be within a predefined narrow range that is specific to each mountain gap location. The expected wind direction range for each study location was determined using years of observed gap wind events in satellite data. The wind direction range for the Tehuantepec, for example, is between 200 and 310 degrees. Different wind ranges are used for each gap region.

Step 6: Calculate wind statistics for the gap wind region

Statistical properties of the grid cells in the identified gap wind region are calculated and recorded. These values include: maximum wind speed, mean and standard deviation of the wind speeds, mean and standard deviation of wind directions, region area, and mean latitude and longitude of the detected region. The recorded values are used for web site display.

Step 7: Combine maps to generate gap wind events

In this final step, we combine results from the individual 6-hourly CCMP maps to determine the temporal extent of a gap wind event. Gap wind events in these regions typically vary in duration, from as short as a single map (6-hours) to as long as multiple weeks. While our intention is to identify the longer, stronger wind events that generate greater SST upwelling events, some strong short-duration events can also exist that cause cold water upwelling, so it is important to identify these as well. We record all the identified gap wind events that last for at least three successive wind maps (a total of 18 hours or more - referred to as 3-map events). Shorter gap wind events that have notably high wind speeds are also recorded. Relatively weak and short events referred to as 1-map events (6 hours) or 2-map events (12 hours) are also examined to determine if they need to be merged with previous or subsequent events.

Wind is a highly variable geophysical parameter and is especially variable in the Central American gulf regions as local-scale coastal winds (i.e. land/sea breezes) increase or decrease the regional winds (gap winds) observed by the satellite instruments. Night-time land breezes blow offshore in the same direction as the gap wind. However, daytime sea breezes blow onshore, opposite the wind jet momentum and therefore can result in a lower wind. The local daytime breezes (10 am to 8pm) occur during the 18z and 0z CCMP maps for this geographic longitude. As a result, winds in these maps may appear lower than our threshold even though a wind jet continues to blow. In these circumstances, the algorithm fails to identify the wind event due to the local sea breeze effect. We have therefore developed a series of rules to handle 1-map events and recover the long duration events that would have been identified if the local sea breeze patterns had not existed. As a consequence, only the true very short duration weak events are excluded from the gap wind climatology.

After performing the combining steps, the gap wind statistics listed below are calculated and preserved in the RASI Climatology dataset at the GHRC, and made available for browsing, analysis and download in the GHRC Regional Air-Sea Interactions (RASI) web environment (see section V).

B. Ocean Upwelling Detection

Gap winds can induce a decrease in SST due to the movement of warm surface water away from the coast, resulting in deeper cold water rising to the surface. Stronger gap wind events can cause significant SST cooling that may last for days or even weeks before the SST warms to typical regional temperatures. Weaker gap winds are often of insufficient strength or last for too short a time to cause measureable cold water upwelling. SST events, therefore, vary in both duration and intensity. Our detection algorithm needs to not only identify cold-water upwelling in a single daily map, but also to accurately determine the start and end points of an SST upwelling event.

Some of the same methodology developed for the wind identification is employed in the detection of SST cold-water upwelling; however there are some significant differences. The detection of cold-water upwelling is a simpler process than the detection of gap winds, partly because the individual SST maps represent a daily SST rather than the 6-hour time span of the CCMP wind data, and also due to the fact that SST varies less in time than the surface wind speeds. Although cold water can surface quickly with strong gap winds, the water typically warms slowly after the cessation of the gap wind event. Since a new SST event can begin before the coastal water has returned to pre-event temperatures, we define the end of an SST upwelling event as the time when the temperature "begins to warm" rather than when the SST returns to its original temperature. This prevents several events from merging together and becoming indistinguishable.

Our SST event detection algorithm locates occurrences of significant temperature decrease over three regions. The three regions we examine are located inside the LargeAreas used in the wind detection methodology. The region at the Gulf of Tehuantepec is shown in Fig. 1 as a green dashed box and is referred to as the SSTArea. In general, the SST upwelling events originate near the coast where the gap winds are strongest. We restrict the regions for SST event detection in order to prevent identifying episodes of SST decrease due to other synoptic weather systems or to surface water freshening during excessive rain. We use an SST reference location outside the SSTArea box to represent the neighboring non-event conditions. The SST reference location is shown in Fig. 1 as a green dot. We require that the start of the SST event not only have an observed decrease in SST, but most significantly, the lowSST must be at least 2 degree Celsius lower than the reference location. We do not perform any temporal merging of individual maps as used in the wind detection methodology since SST is much less temporally variable than wind.

To detect the area of cold water upwelling, we subtract the previous day SST map from the current day SST map and calculate the SST change statistics, focusing on the 16 grid cells with the largest SST decrease. Besides SST decrease statistics (change in SST from previous day), we also estimate the 'coldness' of the SSTArea by calculating the SST statistics of the 16 grid cells with the lowest SST values in the area, including the mean value (lowSST). This mean value (lowSST) indicates how cold the ocean surface is for the day. Though the 16 grid cells used in the low SST and SST decrease calculations may be quite different on non-event days, they are highly related as the cold SST grid cells are essentially caused by the event. No requirement was made that the 16 cells be next to each other, though for SST events, they are expected to be coherent with each other. The statistics calculated are the important discriminators used to identify the beginning of an SST event.

The end of the SST event is selected as the map where the lowSST value of the "next/following" map is higher – indicating that the SST is beginning to recover to pre-event levels.

IV. Wind and SST findings for 1997 to 2012

The above methodologies were used to process over 10 years of CCMP wind and MWOI SST data for the three gulf regions. During the methodology development phase, individual daily and yearly results were spot checked to ascertain whether reasonable results were obtained. The findings show that the Gulf of Tehuantepec has the highest gap wind speeds, and not surprisingly, the strongest ocean upwelling also with decreases in SST up to 7 deg C. The Gulf

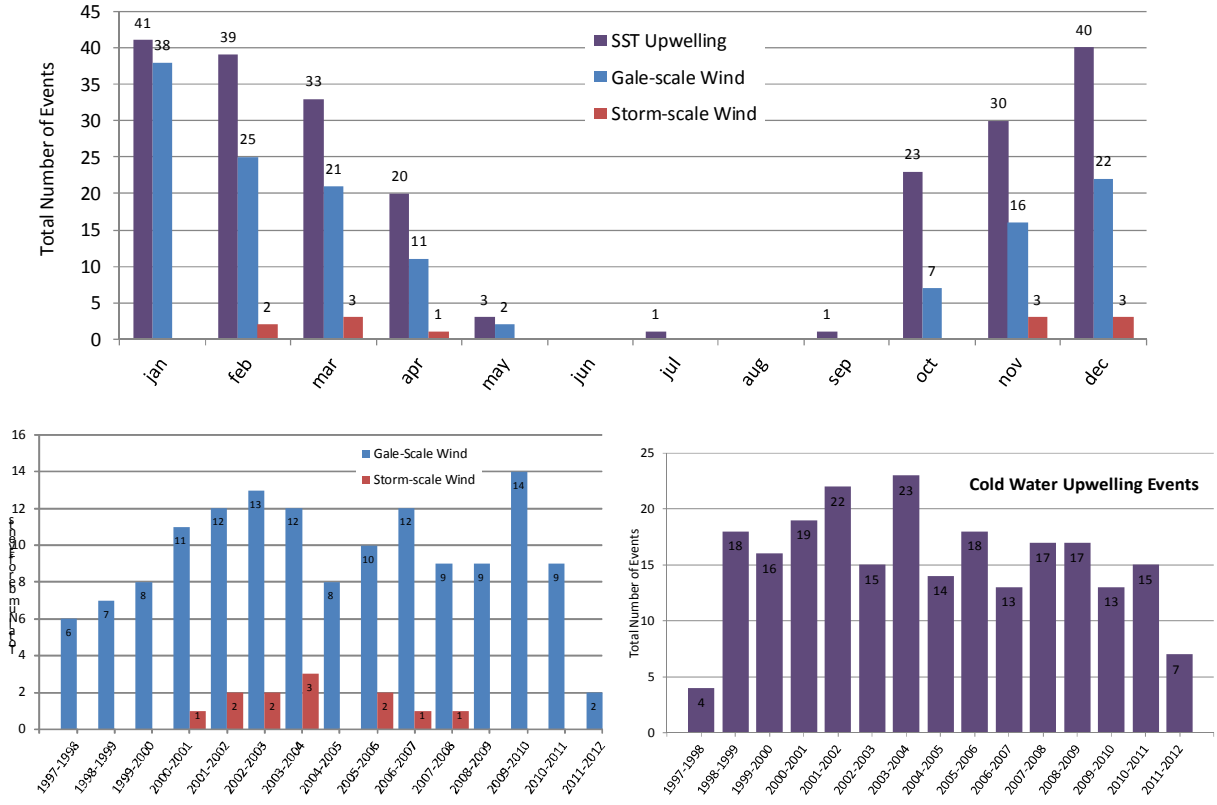

Fig. 2. Plots of the total number of wind and ocean upwelling events by month (top) and the total number of wind (left) and SST (right) events by years (bottom) for all years processed. Years start Oct 1 in order to fully represent cold seasons when the events typically occur. Both the 1997-1998 and 2011-2012 were partial seasons due to limits on data availability (January 1998 to December 2011).

of Papagayo has more days of wind and SST events than the other two regions. For this presentation, we have focused on the Gulf of Tehuantepec results, but similar results for the Gulfs of Papagayo and Panama can be examined online (see next section).

Fig. 2 shows the total number of wind event and ocean upwelling event statistics by month (top) and for the years 1997 to 2012 (bottom) for the Gulf of Tehuantepec. The general understanding that wind and associated ocean upwelling events occur primarily in the winter months is demonstrated and looks similar to results found by Brennan et al. (hereafter referred to as Brennan)[10]. A direct comparison of our results with those of Brennan for the Gulf of Tehuantepec is difficult to make since that study exclusively used QuikSCAT wind data (as opposed to the CCMP product, though CCMP does include QuikSCAT data as one input to the 4D-Var processing) and therefore the products have different temporal and spatial scales which can alter results (2 daily overpasses of QuikSCAT vs. 6-hourly CCMP maps and the use of 12.5 km QuikSCAT winds vs. CCMP 0.25 deg gridded winds).

That said, we make a comparison here to demonstrate that our automated methodology works and can adequately detect wind and upwelling events to within the range expected from the data source differences. Table 1 shows the results of the total number of cold season gale and storm wind events for both our study and Brennan. The number of gale-scale events is similar, but we find far fewer storm-scale events, likely due to the spatial resolution of the data. Table 2 shows the mean number of gale and storm events for the ten cold seasons from 1998 to 2012 and for the 3 cold seasons from 1999 to 2002 as reported in Cobb et al. [21]. Given that Brennan saw an increase in storm-scale events when they switched from 25 km QuikSCAT data to 12.5 km data, we expect the lower number of storm-scale events as shown here, but expect better agreement with Cobb. The most remarkable disagreement is that Brennan found January had the greatest number of storm-scale events we found 0 events for Jan. On inspection, we did find storm-scale winds, but they belonged to an event that started on Dec 31st of the year before and was not counted in the Jan results.

The maximum decrease in SST in the study area during ocean upwelling events was approximately 7 deg C. This result is similar to that determined by Schultz et al. [22] and many earlier studies mentioned within.

An important result of our analysis is the relationship of the ocean upwelling to the gap wind jet occurrences. We find that the percentage of days identified as having a wind event which also has an associated SST cooling is approximately 29%. However, the percentage of upwelling events with associated gap winds blowing is 98%. So roughly 1/3 of the windy days are either strong enough or last long enough to produce cold water upwelling, but the cold water upwelling in this region primarily occurs only due to this important regional gap wind. Since the cold water upwelling also brings up nutrients essential to fish communities, monitoring changes in gap wind patterns is essential. The monthly plot of Fig. 2 may seem contradictory to these statistics as it shows many more upwelling events than wind events per month however this is solely due to our definition of an upwelling event. Each of these events do have a related wind event.

TABLE I. COMPARISON OF TOTAL NUMBER OF COLD SEASON (OCT TO MARCH) GAP WIND EVENTS FOR 1999 TO 2009

	Total Gale Events (1999-2009)	**Total Storm Events (1999- 2009)**
this analysis	110	12
Brennan et al.	119	64

TABLE II. MEAN NUMBER OF EVENTS FOR THE GULF OF TEHUANTEPEC FOR THIS STUDY AND AS REPORTED IN THE LITERATURE

	Avg # Gale Events	**Avg # Storm Events**
10 cold seasons, 1999 to 2009 (this analysis / Brennan)	11 / 12	1.2 / 6.4
3 cold seasons, 1999 to 2002 (this analysis / Cobb)	10 / 15	0.5 / 2

RASI CLIMATOLOGY DATA ACCESS

The DISCOVER project is a collaboration that includes the NASA Global Hydrology Resource Center (GHRC) at the Marshall Space Flight Center (MSFC). The GHRC is a NASA distributed active archive center (DAAC) and is jointly managed and operated by the MSFC Earth Science Division and the UAH Information Technology and Systems Center (ITSC). The RASI climatology is archived and managed by the GHRC for the DISCOVER project. Access to the RASI information is being provided through a special web application interface designed to allow users to browse both the event occurrences as well as the actual data (see Fig. 3).

A. View Individual Maps

The temporal nature of the event occurrences is visualized on a calendar interface (View Events) that allows users to quickly navigate dates to compare monthly and yearly patterns of both gap wind and ocean upwelling events from any of the three mountain gap locations in this study. The wind and SST event bars on the calendar interface (see Fig. 3) are also links to images of the corresponding CCMP and SST data that were used for the identification of that day's events, allowing the user to visually verify the event that the algorithm has identified.

B. Get or Plot Time Series Data

A data access and analysis tab on the web application (Get or Plot Data) provides users with the ability to view and download all the climatology parameters, subsetted for a specific date range. Additionally, the application allows users to create a variety of plots of the climatology parameters against time to quickly view and compare trends and patterns in the data across years, seasons, etc. The climatology parameters include wind speed maximums and means, and reference point values for gap wind events, as well as SST maximum decrease, minimum, mean and reference point values for the SST upwelling events.

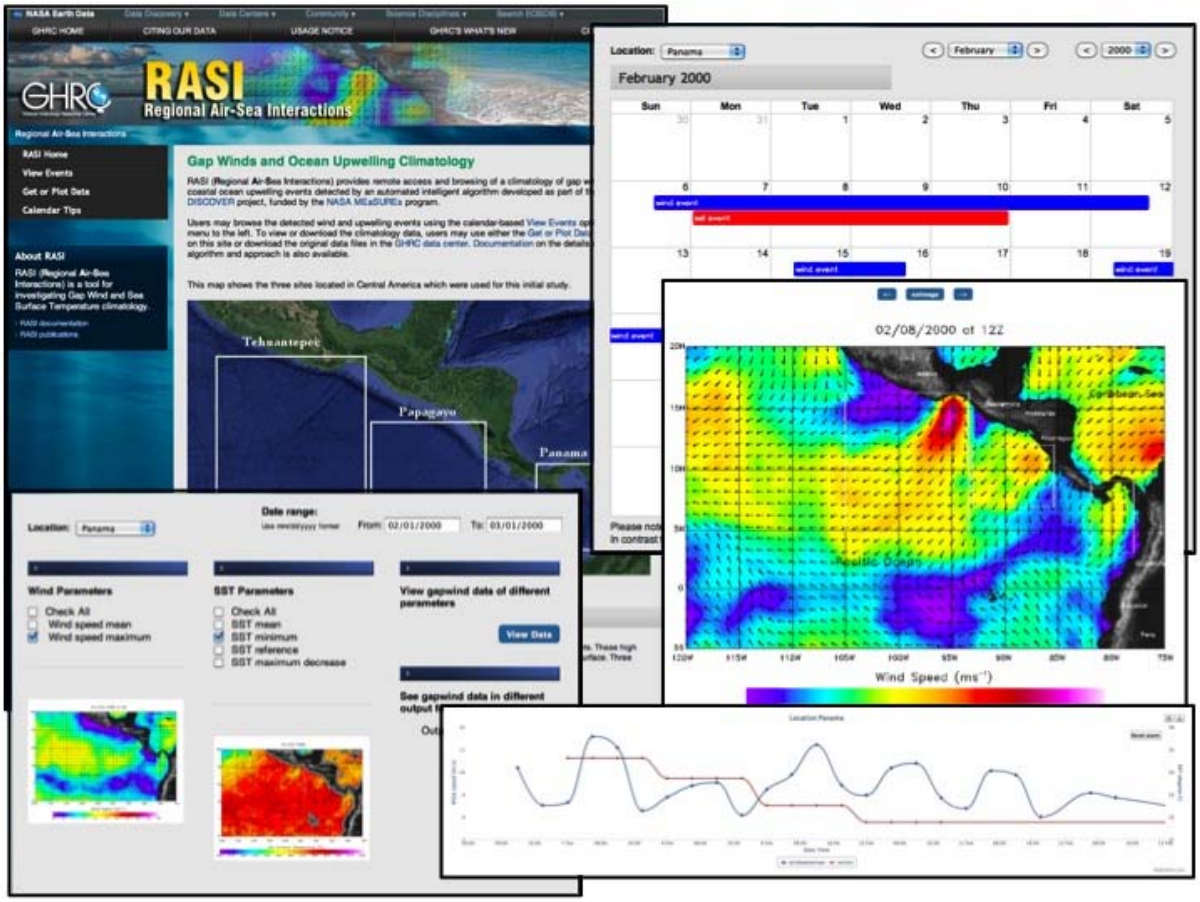

Fig. 3: Example RASI web application tools displaying temporal view of event occurrences and data plotting and access.

The RASI data is open and publicly available for researchers from the GHRC-hosted web application (https://ghrc.nsstc.nasa.gov/rasi/main.php). Detailed documentation of the algorithms described in this paper are available at the RASI site, as well as specific instructions on the visualization and data access tools provided at the site. We welcome feedback and suggestions from users on how to improve the usefulness of this site to support the use of the RASI climatology.

V. Summary

This document presents the wind and SST algorithms used to automatically identify gap wind and SST upwelling events from years of satellite wind and SST data for three gulf regions located in Central America. Hierarchical thresholding along with a number of rules are used to identify gap wind regions from CCMP wind maps. Successive maps in which gap winds are located are then merged to determine the start and end of the entire gap wind event. Cold water upwelling which may be associated with gap wind events are identified from MW OI SST data by locating regions with significant SST decrease as compared to previous day values. The identified SST events end when SST values in the region no longer decrease.

Wind and SST data statistics over the identified regions are calculated, including mean and standard deviation with results available to the public via a specially tailored web environment. The RASI Climatology is maintained at the GHRC and event information can be viewed, analyzed and downloaded at the RASI web interface.

Analysis of our findings show reasonable agreement with previous findings suggesting that the methodologies developed function to within a range permissible by the spatial and temporal resolution of the data used.

Acknowledgment

The authors wish to thank NASA for funding this work through the NASA/MEaSUREs project.

References

[1] W.J. Steenburgh, D.M. Schultz, and B.A. Colle, 1998: The structure and evolution of gap outflow over the Gulf of Tehuantepec, Mexico. Mon. Wea. Rev., vol. 126, pp.2673-2691.

[2] D.B. Chelton, M.H. Freilich, and S.K. Esbensen, 2000a: Satellite observations of the wind jets off the Pacific Coast of Central America.

Part I: Case studies and statistical characteristics. Mon. Wea. Rev., vol. 128, pp. 1993-2018.

[3] L.T. Chapel, 1927: Winds and storms on the Isthmus of Panama. Mon. Wea. Rev., vol. 55**,** pp. 519–530.

[4] W.E. Hurd, 1929: Northers of the Gulf of Tehuantepec. Mon. Wea. Rev*.,* 57**,** 192–194.

[5] R. Legeckis, 1988: Upwelling off the Gulfs of Panama and Papagayo in the Tropical Pacific during March 1985. J. of Geophy.Res., vol. 93, pp. 15485-15489.

[6] A.J. Clarke, 1988: Inertial wind path and sea surface temperature patterns near the Gulf of Tehuantepec and Gulf of Papagayo. J. Geophy. Res., vol. 93, pp. 15491-15501.

[7] H.G. Stumpf, 1975: Satellite detection of upwelling in the Gulf of Tehantepec, Mexico, J. Phys. Ocean., vol. 5, pp. 383-388.

[8] D.B. Chelton, M.H. Freilich, and S.K. Esbensen, 2000b: Satellite observations of Central American coastal wind jets. Part II: Regional relationships and dynamical considerations. Mon. Wea. Rev*,* vol. 128**,** pp. 2019–2043.

[9] S-P. Xie, H. Xu, W.S. Kessler and M. Nonaka, 2005: Air-sea interaction over the Eastern Pacific Warm Pool: Gap winds, thermocline dome, and atmospheric convection, J. of Climate, vol. 18, pp. 5-20.

[10] M.J. Brennan, H.D. Cobb, and R.D. Knabb, 2010: Observations of the Gulf of Tehuantepec gap wind events from QuikSCAT: An updated event climatology and operational model evaluation. Weather and Forecasting, vol. 25, pp. 646-658.

[11] X. Li, D.K. Smith, K. Keiser, Automated detection of gap wind and ocean upwelling events in Central American gulf regions. In: 92nd American Meteorological Society Annual Meeting. 92nd American Meteorological Society Annual Meeting. New Orleans, LA; 2012.

[12] D.B. Chelton, M.G. Schlax, M.H. Freilich, and R.F. Milliff, 2004: Satellite measurements reveal persistent small-scale features in ocean winds. Science, vol. 303, pp. 978–983.

[13] R.M. Atlas, R.N. Hoffman, J. Ardizzone, S.M. Leidner, J.C. Jusem, D.K. Smith and D. Gombos, 2011: A cross-calibrated, multi-platform ocean surface wind velocity product for meteorological and oceanographic applications, Bull.Amer. Met. Soc.,vol. 92(11), pp. 157-174.

[14] C.L. Gentemann, F.J. Wentz and M. DeMaria, 2006: Near real time global optimum interpolated microwave SSTs: Applications to hurricane intensity forecasting, paper presented at the AMS 27th Conference on Hurricanes and Tropical Meteorology, Monterey, CA.

[15] A.Z. Arifin and A. Asano, 2006: Image segmentation by histogram thresholding using hierarchical cluster analysis, Patt. Recog.Lett., vol. 27(13), pp. 1515-1521.

[16] J.E. Peak, and P.M. Tag, 1994: Segmentation of satellite imagery using hierarchical thresholding and neural networks, J. App. Met., vol. 33, pp. 605-616.

[17] C.W. Yang, P.C. Chung, and C.I. Chang, 1996: Hierarchical fast two-dimensional entropic thresholding algorithm using a histogram pyramid, Optical Engineering, vol. 35(11), pp. 3227-3241.

[18] N. Otsu, 1979: A threshold selection method from gray-level histograms, IEEE Trans.Sys., Man, and Cyb.,vol. 9(1), pp. 62–66.

[19] J. Canny, 1986: A computational approach to edge detection, IEEE Trans. Patt.Anal. and Mach. Intell., vol. 8(6), pp. 679–698.

[20] R.C. Gonzalez and R.E. Woods, 1992: Digital Image Processing, *Addison-Wesley Publishing Company*, 716pp.

[21] H.D. Cobb, III, D.P. Brown, and R. Molleda, 2002: Use of QuikSCAT imagery in the diagnosis and detection of Gulf of Tehuantepec wind evetns 1999-2002. Paper presented at the 12th Conf. on Satellite Metoeorology and Oceanography, Long Beach, CA, Amer. Meteor. Soc., JP4.1. [Available online at http://ams.confex.com/ams/pdfpapers/54957.pdf]

[22] D.M. Schultz, W.E. Bracken, and others, 1997: The 1993 superstorm cold surge: Frontal structure, gap flow, and tropical impact. Mon. Wea. Rev., vol. 125, pp. 5-39.